DIFFUSER PERFORMANCE OF A MACH 6 OPEN-JET TUNNEL AND MODEL-BLOCKAGE EFFECTS AT STAGNATION TEMPERATURES TO 3,600° F

By Raymond E. Midden and Bennie W. Cocke, Jr.

Langley Research Center
Langley Station, Hampton, Va.

NATIONAL AERONAUTICS AND SPACE ADMINISTRATION

For sale by the Office of Technical Services, Department of Commerce,
Washington, D.C. 20230 -- Price $0.75

DIFFUSER PERFORMANCE OF A MACH 6 OPEN-JET TUNNEL AND MODEL-BLOCKAGE EFFECTS AT STAGNATION TEMPERATURES TO 3,600° F

By Raymond E. Midden and Bennie W. Cocke, Jr.
Langley Research Center

SUMMARY

A diffuser evaluation program was conducted to develop an effective fixed-area diffuser for a Mach 6 open-jet wind tunnel. In this program several diffuser parameters were varied and evaluated in terms of empty-jet starting efficiency and running efficiency with blunt models and support systems inserted in the airstream. Permissible model blockage for tunnel operation was defined for several variations of the diffuser parameters.

Test results show that good recoveries can be obtained with the fixed-area diffuser, and that blunt models (hemispheres) with up to 18-percent blockage can be operated in a tunnel with a properly designed diffuser. Investigation also shows that operation with blunt models requires the use of second-minimum area ratios appreciably larger than the optimum empty-jet values. Furthermore, better efficiencies were obtained with short free-jet lengths and second-minimum sections over 4 diameters in length.

INTRODUCTION

The study of materials and aerodynamics problems associated with reentry and high-speed flight has created a need for ground-test facilities capable of producing high temperature and high Mach number airstreams. In order to extend capability for high-temperature materials research, an 11-inch Mach 6 nozzle, test section, and diffuser were built and adapted to an existing 3,600° F zirconia pebble-bed heat exchanger for the primary purpose of high-temperature materials research.

This Mach 6 system was designed using a water-cooled axisymmetric conical nozzle, a free-jet test section, and a short fixed-geometry diffuser exhausting to the atmosphere. A free-jet test section was chosen for this facility from the consideration of operating temperature which made it imperative to be able to insert and retract models from the stream during the tunnel operations.

Initial design of the test section and the diffuser was based on reference 1 and unpublished data from similar free-jet systems. Successful tunnel starts were

obtained with this initial design; however, tunnel flow could not be maintained when blunt models were inserted into the airstream. Since data for model-blockage effects on diffuser design parameters for this type of facility were not available in existing literature, a limited program was undertaken to develop a fixed-geometry diffuser that would allow flow to be maintained when large blunt models were inserted into the airstream.

In this program several diffuser parameters were varied and evaluated in terms of effects on empty-jet starting pressure and running pressure requirements when blunt-nose models and support systems were inserted into the airstream. The parameters varied were second-minimum area ratio, scoop angle, free-jet length, location of second minimum, and length of second minimum. Tests were made for a range of tunnel stagnation temperatures from 2,200° F to 3,600° F and data included flow photographs and Mach number surveys of the tunnel airstream.

This report presents the results from this program and also includes a brief description of the Langley 11-inch ceramic-heated tunnel and its test capabilities.

SYMBOLS

A_1	area of nozzle exit
A_2	area of diffuser second-minimum section
A_B	frontal area of model
D	diameter
D_1	nozzle exit diameter (10.6 in.)
D_2	diffuser second-minimum diameter
D_3	diffuser-scoop entrance diameter (15 in.)
l_1	distance from nozzle exit to diffuser entrance scoop
l_2	length of diffuser constant area (second minimum) section
l_3	length from nozzle exit plane to start of diffuser second-minimum section
M	Mach number
p_E	pressure at diffuser exit (atmospheric)

p_o stagnation chamber pressure, lb/sq in. abs

p_s local static pressure

p_{t_1} total pressure ahead of normal shock (assumed equal to p_o)

p_{t_2} total pressure measured behind a normal shock (model stagnation-point measurement)

r radius

T_o stagnation temperature, ^oF

APPARATUS AND TESTS

11-Inch Tunnel System and Models

The Langley 11-inch ceramic-heated tunnel for which this program was conducted consists of a high-pressure air supply, a heat exchanger, a water-cooled nozzle, a free-jet test section, and a fixed-geometry diffuser exhausting to the atmosphere. These components are shown in figure 1, and a photograph of the nozzle, test section, and diffuser is shown in figure 2.

Heat exhanger.- The heat exchanger consists of a 54-inch-diameter pressure vessel approximately 30 feet tall which is lined with ceramic material and filled with zirconia pebbles as illustrated in figure 1(a). During operation the pebble bed is heated by firing the gas burner until the desired bed temperature is reached. The burner is then turned off and air is brought in at the bottom to pressurize the vessel and to start the blowdown through the nozzle system located on top of the heat exchanger. This ceramic heat exchanger which is described in detail in reference 2 is capable of heating 10 lb/sec of air to an initial temperature of 3,600° F.

Nozzle.- The nozzle used for this system is shown in figure 1(b). This nozzle is a water-cooled conical nozzle with an 8° half-angle expansion and a 10.6-inch-diameter exit. It was designed for an exit Mach number of 6 at 3,600° F air temperature. This nozzle is capable of operation at a stagnation pressure of 1,200 lb/sq in. abs for an air temperature of 3,600° F. The design concepts of the nozzle are presented in reference 2.

Test section.- The free-jet test section is uncooled and incorporates an offset model retraction bay (see fig. 1(b)) for protection of the test model from the thermal environment prior to insertion and after retraction of the model from the airstream. A closure door is provided for the model retraction bay to protect the model during the starting and stopping process of the tunnel. Three observation windows of heat-resistant glass are provided for observing

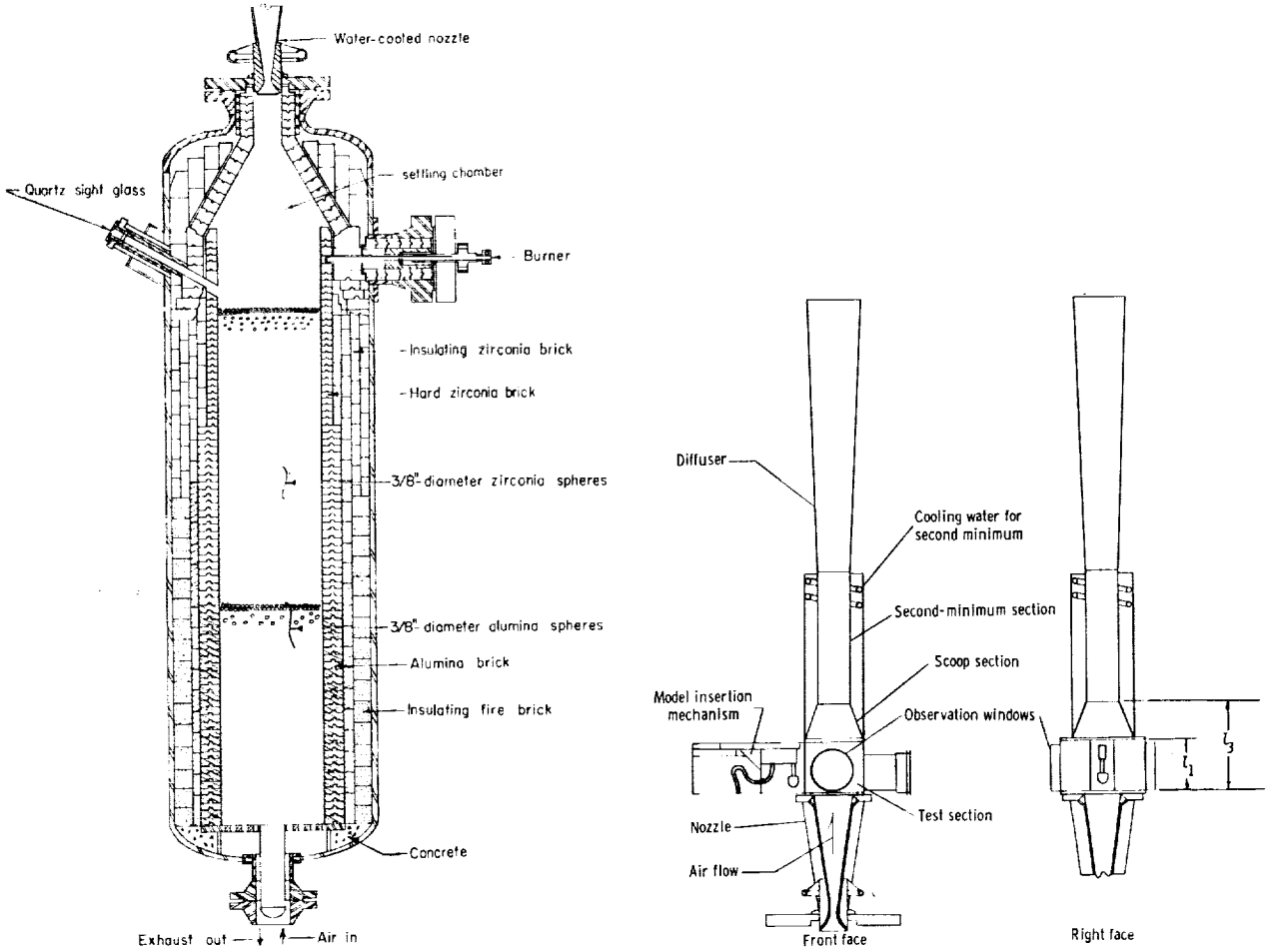

(a) Heat exchanger.

(b) Nozzle, test section, and diffuser.

Figure 1.- Components of Langley 11-inch ceramic-heated tunnel.

the model and for obtaining shadowgraphs of the flow fields. A photograph of the test section and model retraction bay is shown in figure 3. Figure 3(a) shows model retracted and figure 3(b) shows model inserted in the test section.

Diffusers.- Four diffuser configurations, illustrated in figure 4, were studied in this program with several variations of each configuration as indicated in table I. The diffusers evaluated were limited to fixed-area designs and used water spray to cool the second minimum and scoop. These diffuser sections were made of rolled 3/16-inch steel plate welded together. Configuration 1(a) (table I) was based on data in reference 1 and unpublished data which did not include model blockage effects.

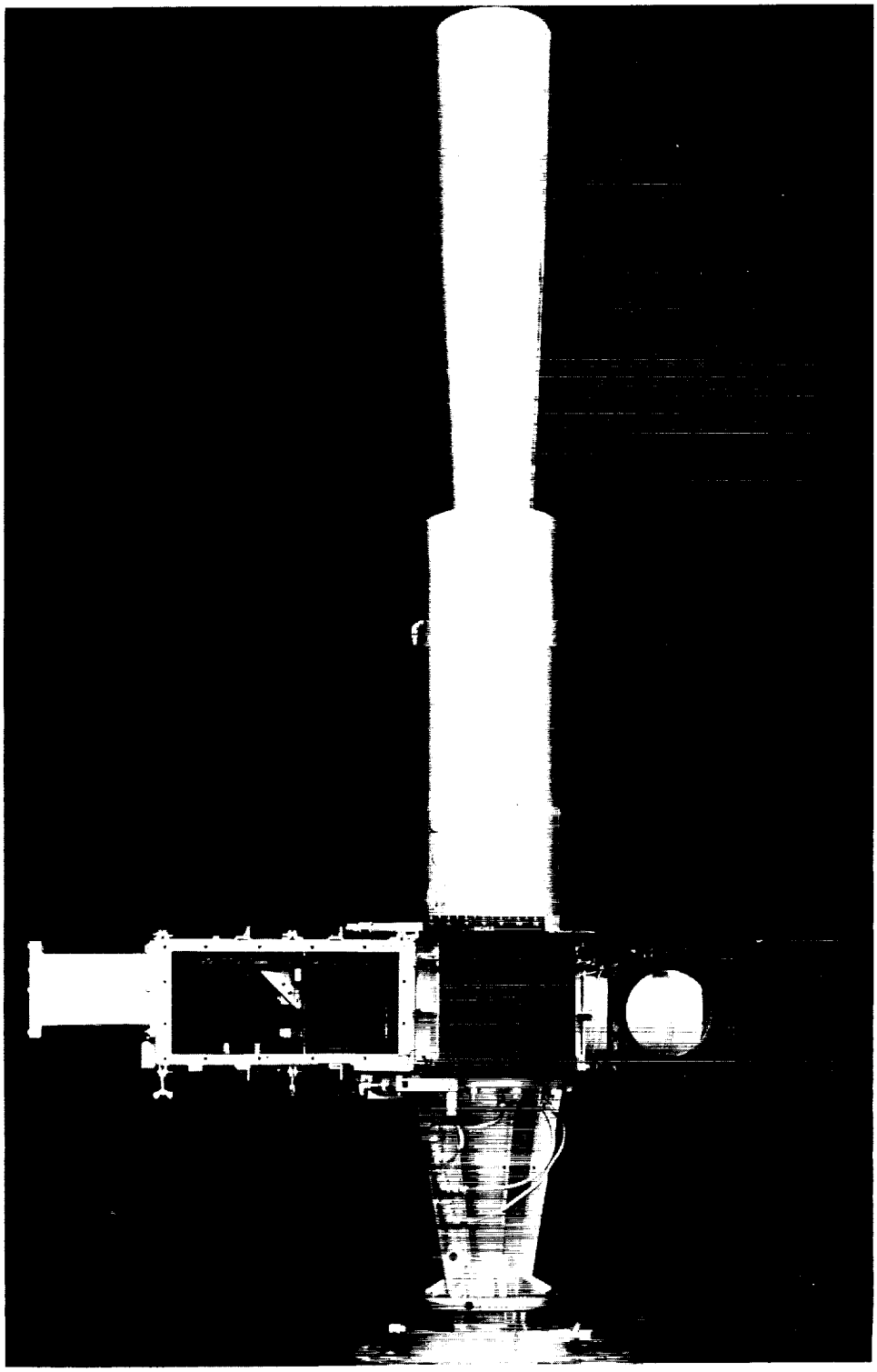

L-64-3023

Figure 2.- Photograph of front face of Mach 6 nozzle, test section, and diffuser.

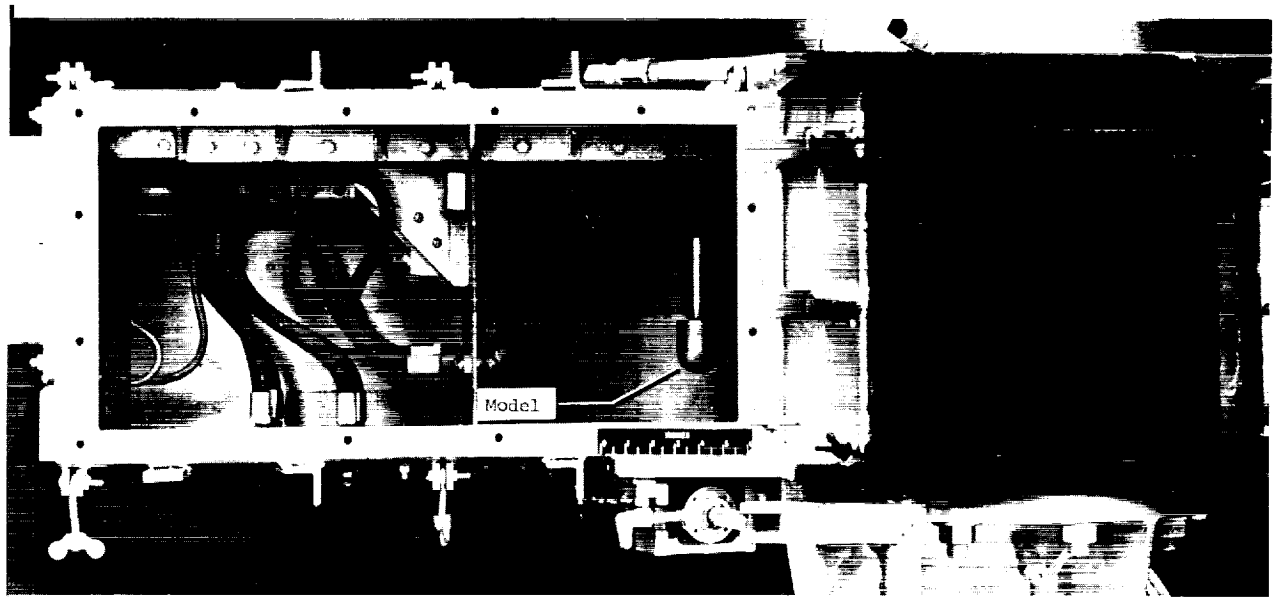

(a) Model retracted. L-64-3024

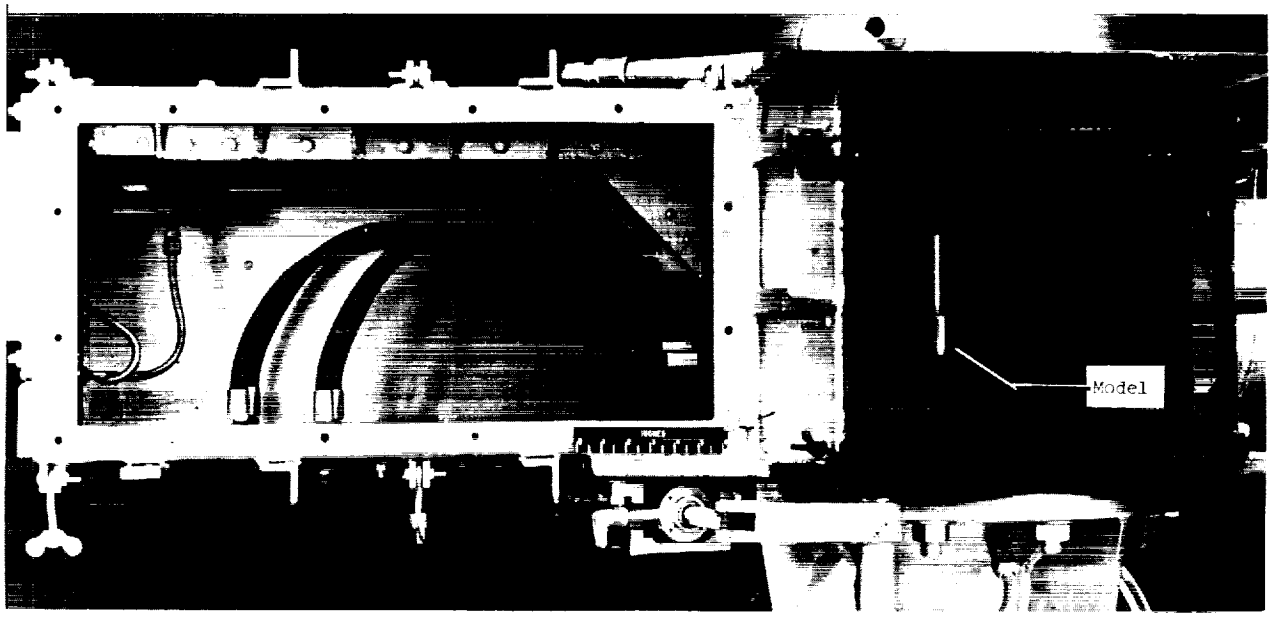

(b) Model in airstream. L-64-3025

Figure 3.- Photograph of test section and model retraction.

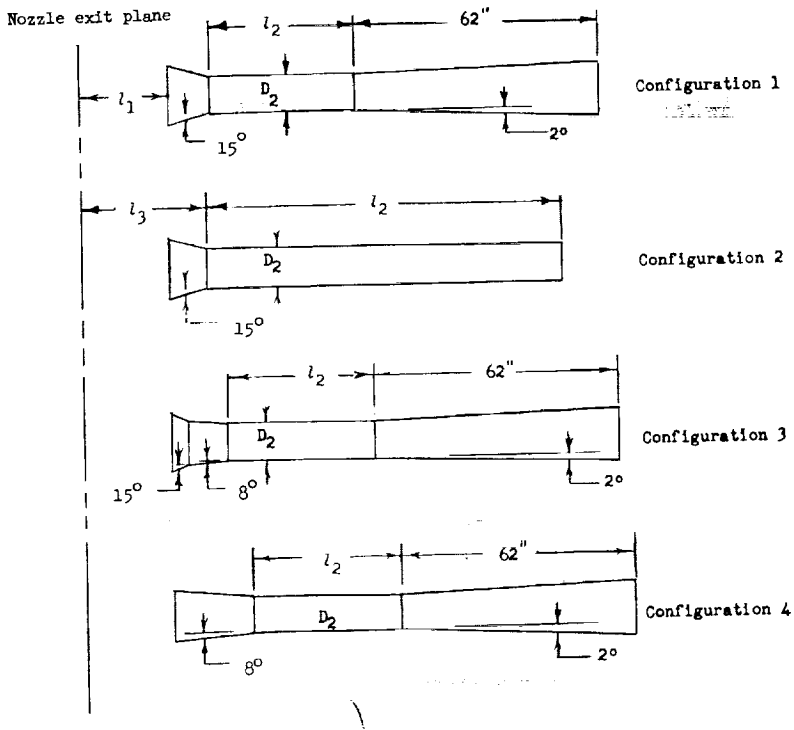

Figure 4.- Diffuser configurations tested.

TABLE I.- DIMENSIONS OF DIFFUSER CONFIGURATIONS

Configuration	l_1, in.	D_2, in.	l_2, in.	l_3, in.	A_2/A_1
1(a)	15.5	8.2	37	28.6	0.60
1(b)	15.5	9.0	37	27.1	0.72
1(c)	15.5	9.5	37	25.6	0.80
1(d)	10.5	9.0	37	21.25	0.72
2	15.5	10.0	90	24.6	0.90
3(a)	15.5	9.0	37	31.75	0.72
3(b)	10.5	9.0	37	26.75	0.72
3(c)	10.5	9.0	17	26.75	0.72
3(d)	10.5	9.0	57	26.75	0.72
4	10.5	9.0	37	32.00	0.72

Models.- To study model blockage effects, three different types of models were used: hemispherical-nose models, flat-faced models, and a 60° conical-nose model. Stagnation-point pressure orifices were incorporated in all hemispherical models to allow measurement of stagnation pressures p_{t_2} during blockage tests. Figure 5 is a sketch of all the models tested. Figure 6 shows typical installation for models in the test section during the run. The nose of each model was mounted $3\frac{3}{4}$ inches from the nozzle exit plane and the strut

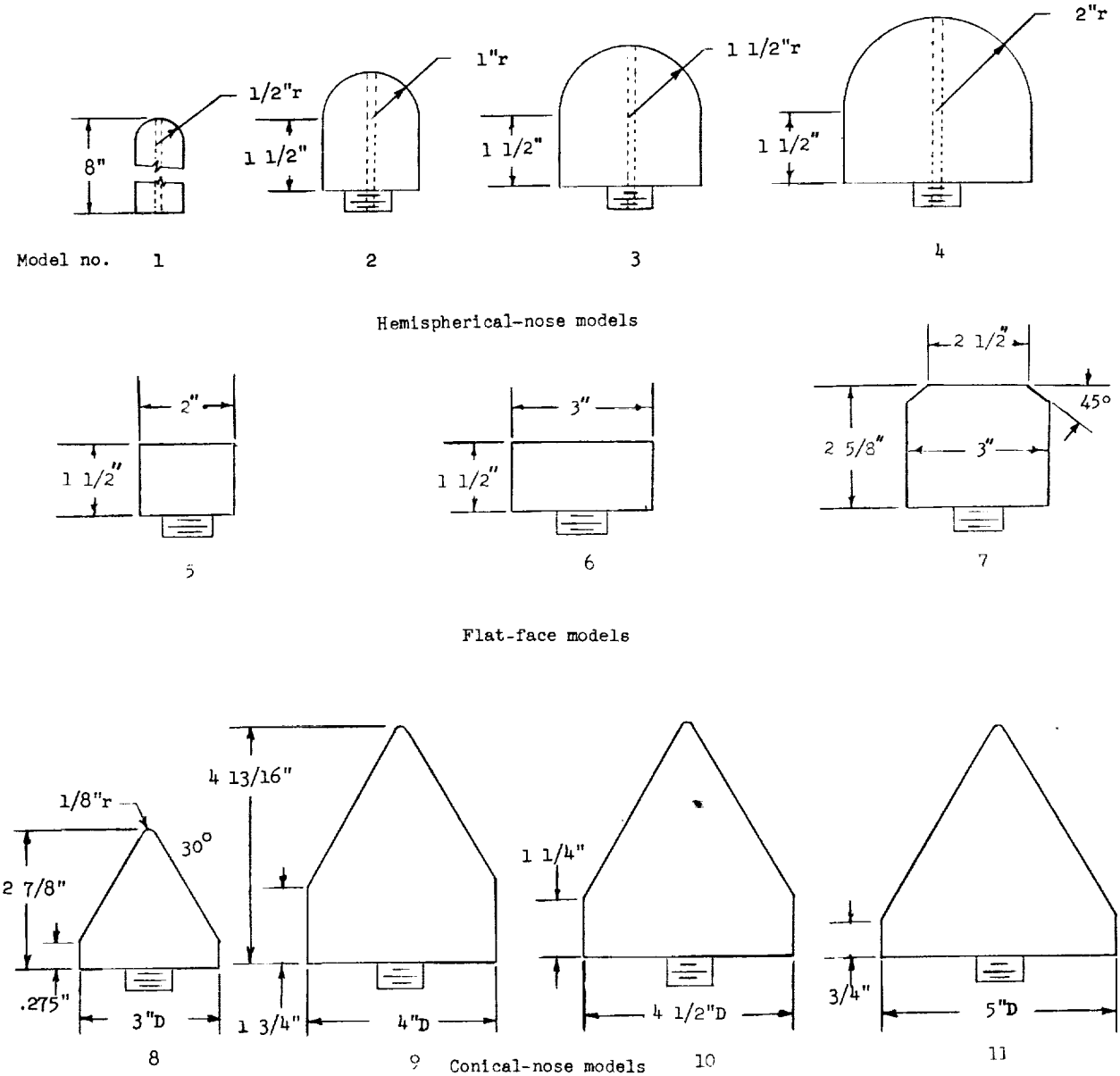

Figure 5.- Details of blockage models.

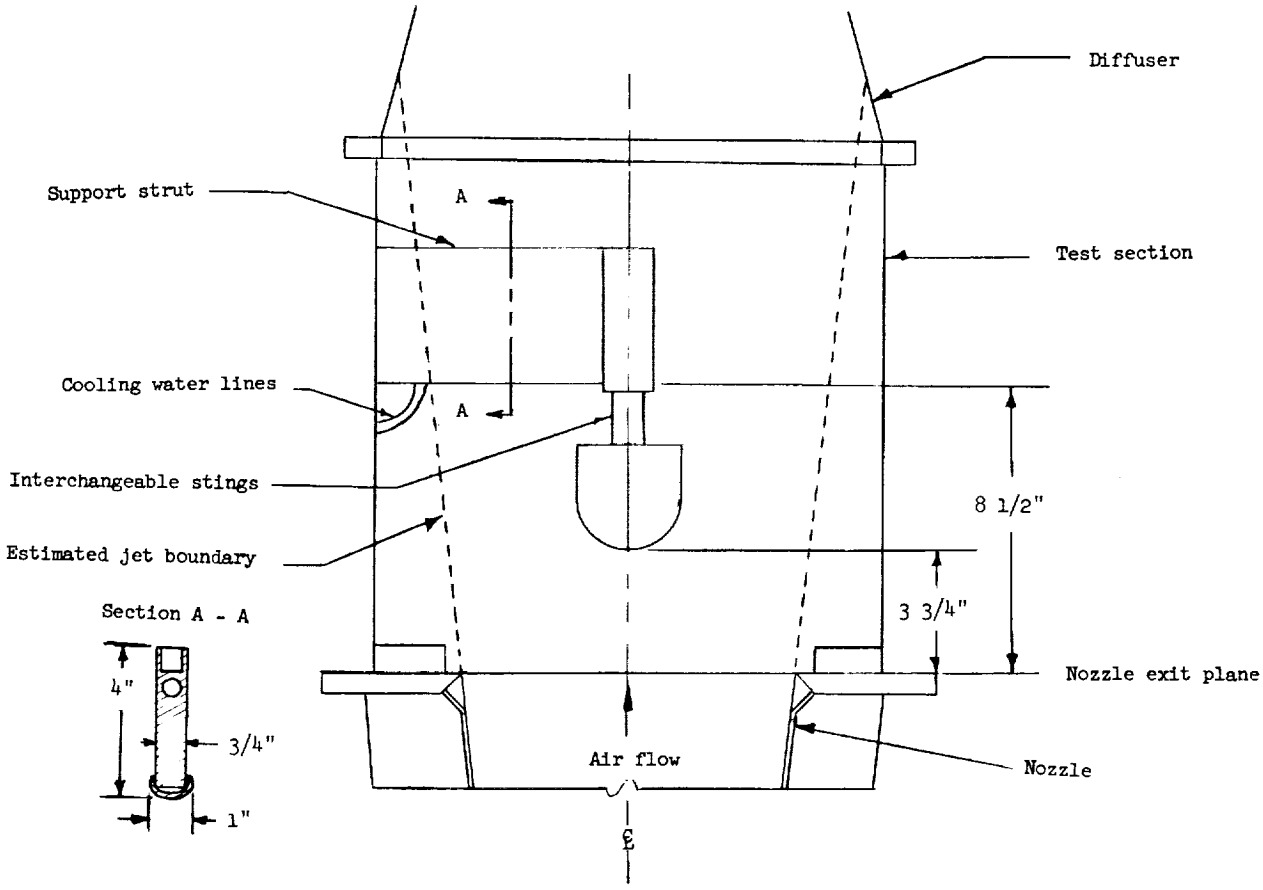

Figure 6.- Typical model installation in test section.

leading edge was mounted $8\frac{1}{2}$ inches from the nozzle exit plane. The models and strut were kept at the same location to eliminate any effect of model position. Struts with blunt leading edges were used during the program and a cross-sectional view of a typical strut is shown in figure 6. Variable length stings were used for each model.

Tests

During this investigation minimum pressure required for starting the tunnel and maintaining flow was measured for each diffuser configuration with and without models in the airstream. In a typical test the 2-inch-diameter hemisphere model (fig. 5, model no. 2) was installed in the retracted position and a given diffuser configuration was installed on the test section. To start the tunnel, the stagnation pressure was gradually increased (from 0 lb/sq in. gage) until the design Mach number was abruptly established in the test section. Flow establishment was indicated by a decrease in test-section static pressure to a steady value approximately equal to the stream static pressure at the design Mach number. After the tunnel started the pressure was generally increased to

700 or 800 lb/sq in. abs and the model was inserted into the airstream. If the tunnel lost flow, the model was retracted and the pressure was increased. If the tunnel flow could not be maintained for the model at 1,000 lb/sq in., the upper limit for routine operation of the facility, the diffuser configuration was removed and another diffuser configuration installed. If the tunnel maintained flow at low stagnation pressures, the model was taken out and a more severe blockage model installed. Installation was done with successively more severe blockage models until the limiting model size for tunnel operation was defined. For the best diffuser configuration tested, stagnation temperatures were varied from 2,200° F to 3,600° F; but most tests were made at approximately 2,800° F.

Measurements and Accuracy

Stagnation pressure, test-section static pressure, and shadowgraphs were recorded throughout the test duration. In addition, for configuration 3(b) wall static pressure distributions were recorded from orifices in a line from the inlet scoop through the diffuser system to the atmospheric exit. Also, several lateral and longitudinal Mach number surveys were made by using a total pressure survey rake, and model stagnation pressure p_{t_2} was measured on the hemispherical models.

The temperature of the top of the pebble bed was read with an optical pyrometer before each run and previous calibration was used to obtain stagnation temperature. Pressures were measured with electrical transducers and recorded on an oscillograph recorder. Shadowgraphs were taken by a 16-mm motion-picture camera operating at approximately 100 frames per second.

A study of the factors affecting the accuracy of results indicates that the measured quantities are accurate within the following limits:

M, ± 0.12

p_o, ± 20 lb/sq in.

T_o, $\pm 100°$ F

p_s, ± 0.3 lb/sq in.

Pressure at the diffuser exit p_E was measured for the static pressure distribution runs but was not measured for the remainder of the tests; a standard value of 14.7 lb/sq in. abs was used.

RESULTS AND DISCUSSION

Tunnel Flow Definition

Figure 7 shows the tunnel stagnation pressure and test-section static pressure plotted against time for a typical tunnel start. As the stagnation

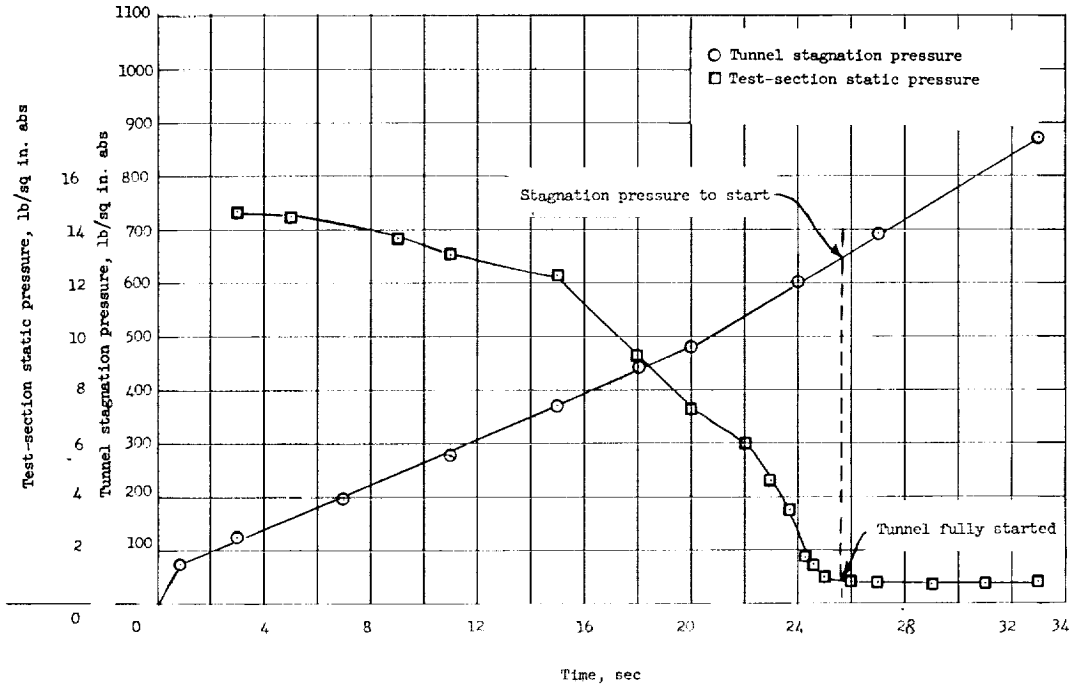

Figure 7.- Tunnel stagnation pressure and test-section static pressure plotted against time during the starting process of the tunnel.

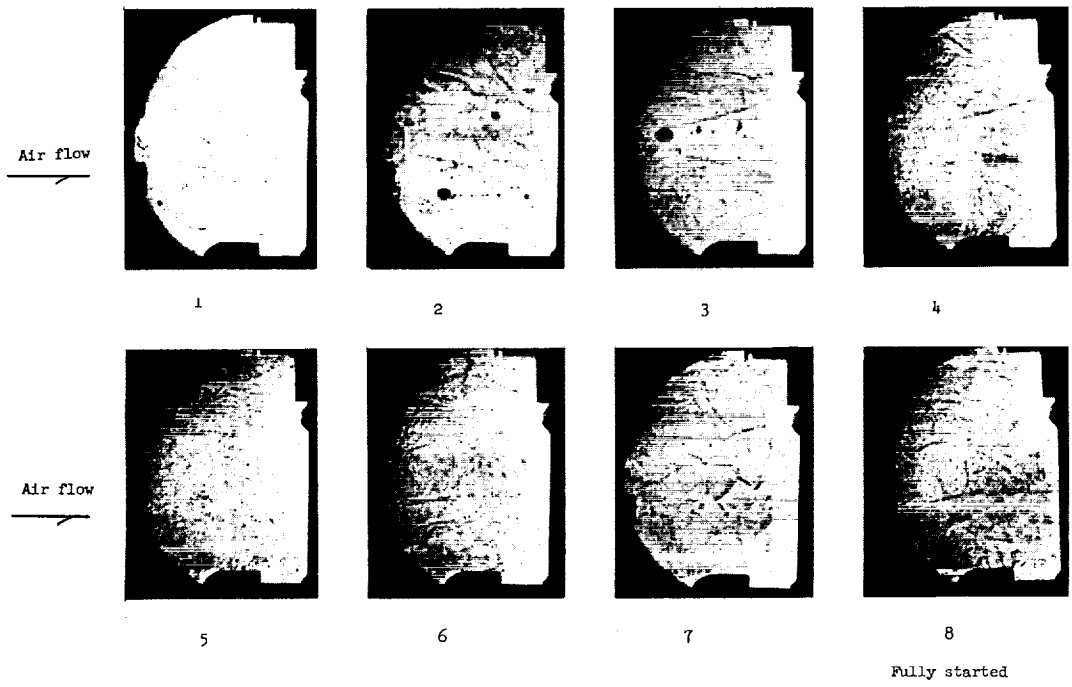

L-64-3026

Figure 8.- Shadowgraphs of starting process of Mach 6 tunnel. (View is through test-section window.)

pressure increased, the test-section static pressure gradually dropped until design Mach number was established in the test section. The tunnel starting was signified by the sharp drop in test-section static pressure to a steady value approximately equal to the stream static pressure.

Figure 8 is a sequence of shadowgraphs taken during a typical tunnel start and shows the shock system as it moves across the test section. This flow pattern is typical of an overexpanded nozzle as the stagnation pressure is increased. The first shadowgraph shows the shock system at the exit of the nozzle. As the stagnation pressure increases, the shock system moves downstream as indicated in shadowgraphs 2 to 7. Finally, when the pressure ratio is sufficient, the shock system moves into the diffuser and the tunnel is fully started as indicated in shadowgraph 8 (fig. 8). These shadowgraphs were taken at approximately 100 frames per second and represent a time interval of approximately 0.1 second in the period between 25 and 27 seconds in figure 7.

Starting pressure for this investigation was defined as the stagnation chamber pressure at the time the test-section pressure reached its minimum value as indicated in figure 7, and starting efficiency was calculated by using the stagnation chamber pressure at the time the tunnel starts for p_o in the following equation:

$$\text{Efficiency} = \frac{p_E/p_o}{p_{t_2}/p_{t_1}} \times 100$$

which relates the minimum pressure ratio p_E/p_o to the normal shock pressure ratio p_{t_2}/p_{t_1} for the operating Mach number. In these calculations, diffuser efficiencies were based on normal shock pressure ratios corresponding to the local Mach number at the normal model position. Mach numbers were computed from total-pressure ratios corrected for temperature effects by using reference 3. In these calculations, an isentropic nozzle flow was assumed and the value of stagnation chamber pressure p_o was used for stream total pressure p_{t_1}. Flow surveys showing the lateral and longitudinal Mach number distribution obtained by the total-pressure surveys in the model test region are presented in figures 9 to 11.

Diffuser Evaluation

The initial diffuser evaluated in this program (table I, configuration 1(a)) was based on unpublished data with compromises to attain maximum length of usable test area (free-jet length l_1) and a minimum overall diffuser length to simplify vertical installation problems on this tunnel. With this diffuser configuration, the tunnel was started at a stagnation chamber pressure of approximately 560 lb/sq in. abs corresponding to a starting diffuser efficiency of 136 percent. These results were in reasonable agreement with design data. However, as summarized in table II, model capability was severely limited and operation with a 1-inch-diameter model required stagnation pressure of approximately 1,000 lb/sq in. abs corresponding to an efficiency of only

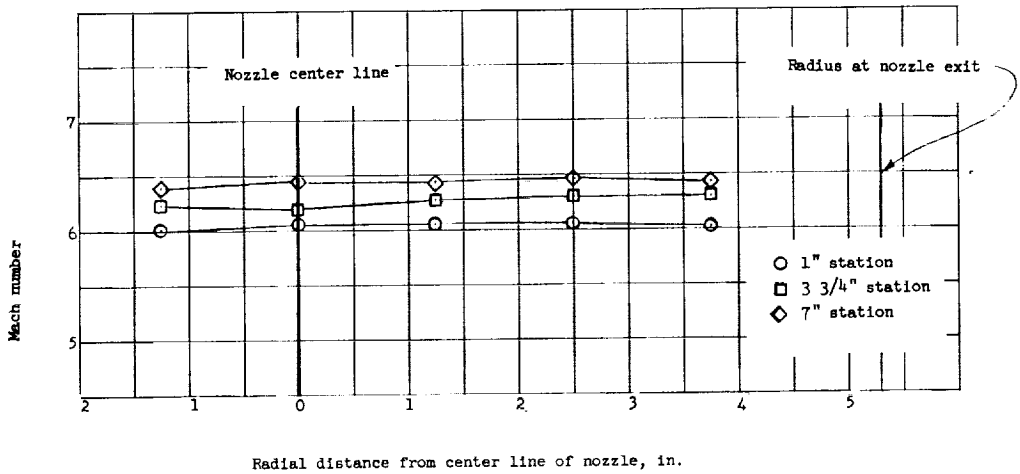

Figure 9.- Mach number distribution across nozzle for three different stations. Temperature, 2,800° F; stagnation pressure, 800 lb/sq in.

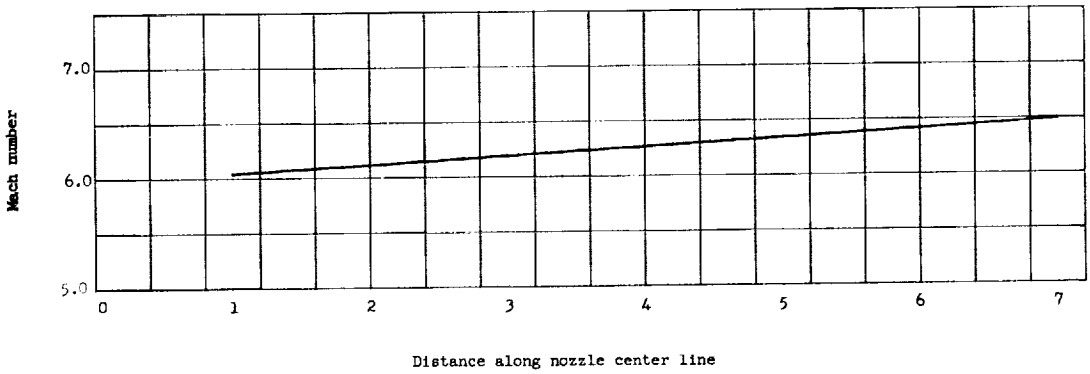

Figure 10.- Variation of Mach number with distance from nozzle exit at 2,750° F.

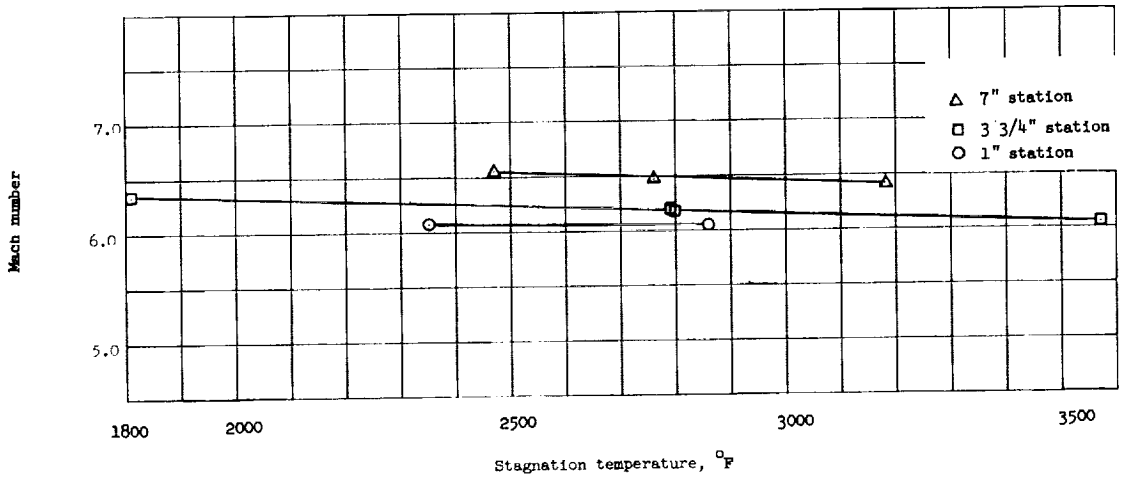

Figure 11.- Variation of center-line Mach number with temperature for three longitudinal stations in test section.

TABLE II.- CHART SHOWING CONDITIONS AT WHICH ALL MODELS WERE TESTED

Model shape	Model diameter, in.	Stagnation temperature, °F	$\frac{A_B}{A_1}$, percent	Stagnation pressure, lb/sq in.	Tunnel flow condition	Model-in running efficiency, percent
Diffuser configuration 1(a); empty-jet starting efficiency, 136 percent						
Hemisphere	1"D	2,335	0.89	800	Flow lost	
Hemisphere	1"D	2,335	.89	1,000	Flow maintained	76
Hemisphere	2"D	2,345	3.56	800	Flow lost	
Hemisphere	2"D	2,345	3.56	1,000	Flow lost	
Diffuser configuration 1(b); empty-jet starting efficiency, 106 percent						
Hemisphere	2"D	2,230	3.56	800	Flow lost	
Hemisphere	2"D	2,210	3.56	1,000	Flow maintained	76
Hemisphere	3"D	2,210	8.0	800	Flow maintained	95
Diffuser configuration 1(c); empty-jet starting efficiency, 103 percent						
Hemisphere	2"D	2,825	3.56	800	Flow lost	
Hemisphere	2"D	2,825	3.56	900	Flow maintained	84.5
Hemisphere	3"D	2,820	8.0	800	Flow lost	
Hemisphere	3"D	2,820	8.0	900	Flow maintained	84.5
Diffuser configuration 1(d); empty-jet starting efficiency, 126 percent						
Hemisphere	2"D	2,140	3.56	800	Flow maintained	95
Hemisphere	3"D	2,260	8.0	700	Flow maintained	108
Flat face	3"D	2,360	8.0	800	Flow lost	
Flat face	3"D	2,360	8.0	1,000	Flow lost	
Flat face	$2\frac{1}{2}$"D	2,310	8.0	800	Flow lost	
Flat face	$2\frac{1}{2}$"D	2,310	8.0	1,000	Flow lost	
Diffuser configuration 2; empty-jet starting efficiency, 89 percent						
Hemisphere	2"D	2,760	3.56	1,000	Flow maintained	76
Hemisphere	3"D	2,790	8.0	900	Flow lost	
Hemisphere	3"D	2,730	8.0	1,000	Flow maintained	76
Diffuser configuration 3(a); empty-jet starting efficiency, 120 percent						
Hemisphere	2"D	2,700	3.56	800	Flow lost	
Hemisphere	3"D	2,260	8.0	800	Flow lost	
Hemisphere	3"D	2,260	8.0	1,000	Flow maintained	76
Diffuser configuration 3(b); empty-jet starting efficiency, 120 percent						
Hemisphere	1"D	2,800	0.89	800	Flow maintained	95
Hemisphere	2"D	2,820	3.56	800	Flow maintained	95
Hemisphere	3"D	2,700	8.0	700	Flow maintained	108
Hemisphere	4"D	2,830	14.2	800	Flow lost	
Hemisphere	4"D	2,830	14.2	1,000	Flow maintained	76
Flat face	2"D	2,745	3.56	800	Flow maintained	95
Flat face	$2\frac{1}{2}$"D	2,745	8.0	800	Flow maintained	95
Cone	3"D	2,350	8.0	800	Flow maintained	95
Cone	4"D	2,745	14.2	700	Flow lost	
Cone	4"D	2,745	14.2	800	Flow maintained	95
Cone	$4\frac{1}{2}$"D	2,810	18.0	1,100	Flow lost	
Cone	5"D	2,760	22.2	1,000	Flow lost	
Diffuser configuration 3(c); empty-jet starting efficiency, 111 percent						
Hemisphere	2"D	2,860	3.56	800	Flow maintained	95
Hemisphere	3"D	2,800	8.0	800	Flow maintained	95
Flat face	$2\frac{1}{2}$"D	2,890	8.0	800	Flow lost	
Flat face	$2\frac{1}{2}$"D	2,890	8.0	1,000	Flow maintained	76
Diffuser configuration 3(d); empty-jet starting efficiency, 126 percent						
Hemisphere	3"D	2,860	8.0	800	Flow maintained	95
Flat face	$2\frac{1}{2}$"D	2,810	8.0	740	Flow lost	
Flat face	$2\frac{1}{2}$"D	2,810	8.0	780	Flow maintained	97
Diffuser configuration 4; empty-jet starting efficiency, 122 percent						
Hemisphere	3"D	2,400	8.0	800	Flow maintained	95
Flat face	$2\frac{1}{2}$"D	2,360	8.0	1,000	Flow lost	

76 percent. Shadowgraphs showing the flow-loss process for a 2-inch-diameter model in this original configuration are presented in figure 12. In this sequence of shadowgraphs, the tunnel is running empty in shadowgraph 1, and shadowgraph 2 shows the flow maintained at the first instant of model insertion. Shadowgraphs 3, 4, 5, and 6 show the loss of Mach 6 flow which occurred within approximately 0.1 second after model insertion. It should be noted that the flow remained supersonic and a shock wave is shown in shadowgraph 6 although the design flow conditions no longer exist in the nozzle system. This condition could be interpreted as a running condition unless model total pressure was measured. As would be expected, a marked increase in heating rate and pressure was noted when this condition existed.

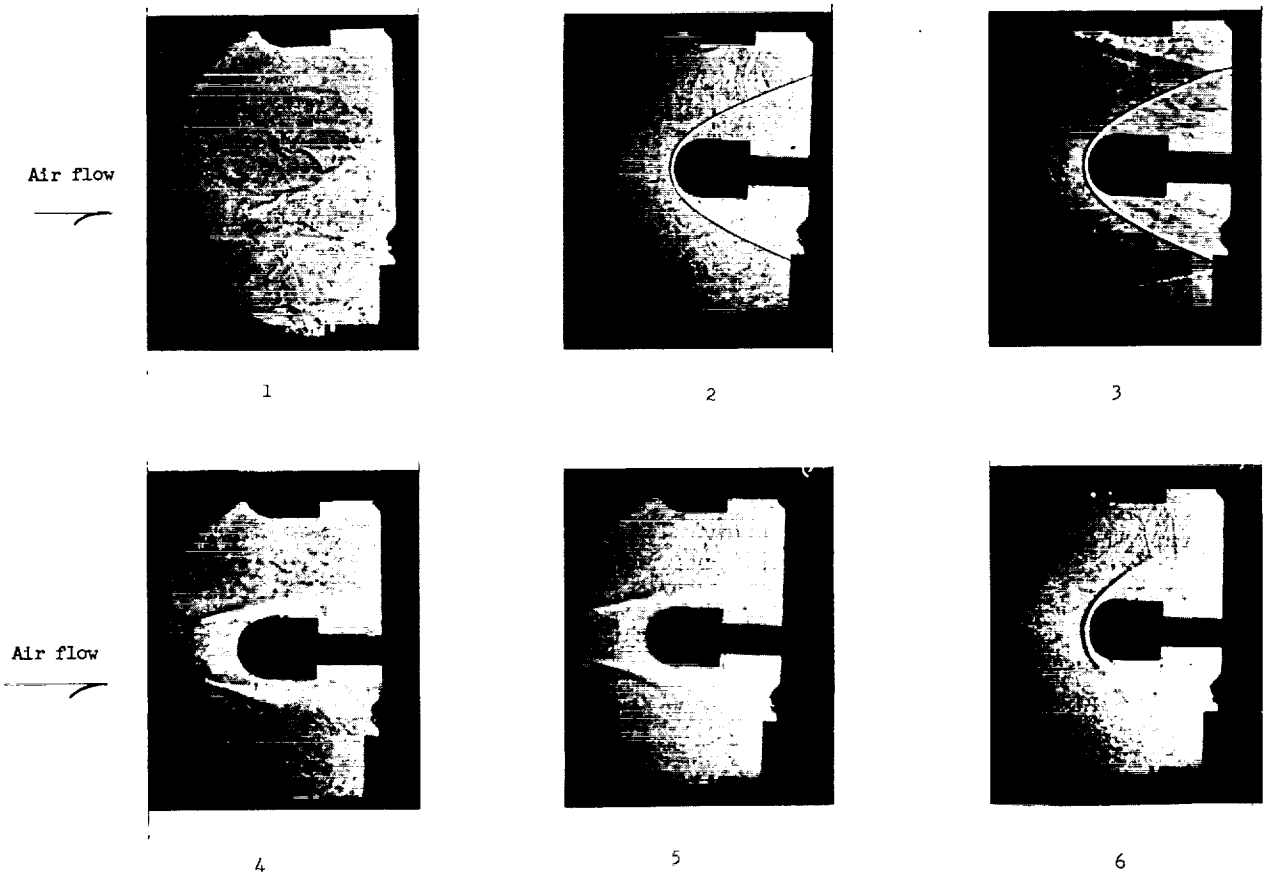

Figure 12.- Shadowgraphs showing loss of design Mach number. L-64-3027

In considering the diffuser variables to be studied for improving model size capability for the tunnel, the data of reference 1 and conventional diffuser concepts were considered. It was felt that most of the diffusion process occurred in the scoop and straight-pipe second-minimum sections; therefore, second-minimum area ratio, scoop configuration, and length of second minimum were the primary variables selected for study.

Effect of second-minimum area ratio.- The results of tests using configurations 1(a), 1(b), and 1(c) (table I) to define the effect of increasing second-minimum area ratio are summarized in figure 13 and table II. As shown by these results, the initial area ratio of 0.6 had the highest efficiency for empty-jet operation of any of the area ratios investigated, yet had the least capability for operating with blunt models. Since the area ratio of 0.6 was near the minimum for starting as predicted by theory (ref. 4), only increases in area ratio were considered. When area ratio was increased to 0.72 (fig. 13), the empty-jet efficiency dropped approximately 21 percent; however, model operating capability was markedly improved. With configuration 1(b), models to 3-inch diameter (blockage of 8 percent) could be run at pressures as low as 700 lb/sq in. abs corresponding to diffuser efficiencies of approximately 98 percent. For larger values of area ratio, empty-jet efficiency continued to decrease and, although the larger models could be run, overall efficiency with model in place was reduced at the higher area ratios.

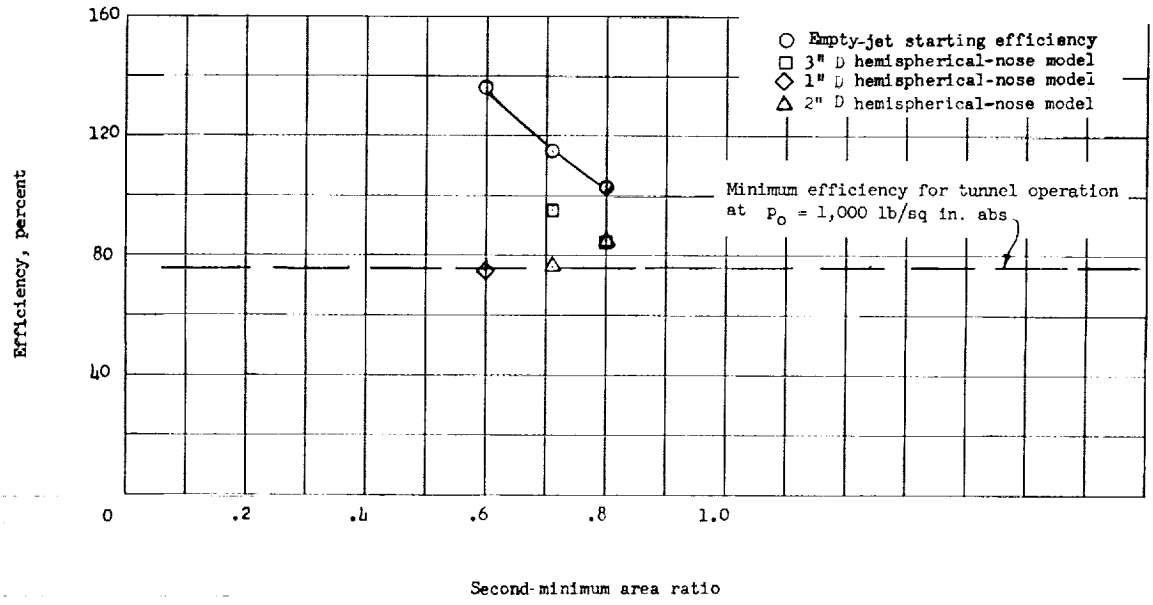

Figure 13.- Effect of second-minimum area ratio on diffuser efficiency for configuration 1.

On the basis of these results it is seen that the area ratio for acceptable model operation in a fixed diffuser must be a compromise, values of approximately 0.7 to 0.75 producing the best overall efficiencies for the diffuser used in these tests. An area ratio of 0.72 was chosen for use in the remainder of this program.

Effect of diffuser-scoop configuration.- In a tunnel of the free-jet type, the diffuser scoop is considered to have several functions. The scoop must collect the flow of the free jet leaving the test region, direct the flow into the second-minimum section, and should accomplish some of the diffusion process in an efficient manner. From these considerations, it is apparent that a number of interrelated geometric parameters should be considered in scoop design.

The ability to collect the flow is dependent on scoop inlet diameter D_3 and free-jet length l_1, and the effectiveness of directing and diffusing the flow should be defined by the scoop contraction angle and the length of the contracting section. As is apparent, these parameters are so geometrically interrelated for an axisymmetric system that it was not possible to isolate all the individual variables in a limited study such as reported herein. Three scoops (fig. 14) were tested, however, and provide indications of the relative importance of the parameters noted. For these scoops, inlet diameter was held constant at the maximum allowable by test-section configuration ($\approx 1.5D_1$), and the exit diameter D_2 was maintained to hold the second-minimum area ratio at the value of 0.72 indicated best in the previous tests. With these limits, scoop angle combinations and free-jet length l_1 became the control variables for the tests conducted. The three scoops (fig. 4, configurations 1, 3, and 4) were obtained by variation of the scoop inlet angle with the aforementioned diameters held constant. As indicated in figure 14, scoops 1 and 3 were tested for two values of free-jet length l_1, and scoop 4 was evaluated only for the shorter free-jet length condition.

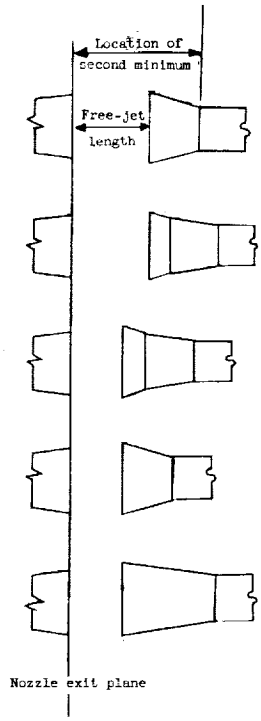

Configuration	Empty-jet starting efficiency	Running efficiency with model in place	
		Model no. 3	Model no. 7
1(b)	115	95	No test
3(a)	120	76	No test
3(b)	120	108	95
1(d)	126	108	Flow lost
4	122	95	Flow lost

Figure 14.- Sketch of configurations used for scoop investigation.

As shown by the test results summarized in figure 14, modifying the scoop angle of the original 15° scoop (configuration 1(b)) to incorporate a two-stage (two-angle) scoop (configuration 3(a)) resulted in a slight increase in empty-jet starting efficiency for the longer free-jet length; however, the running efficiency with hemispherical models in place was reduced. Since the two-stage scoop design results in an increased distance to the start of the second minimum l_3, these data appeared to substantiate previous reports (ref. 5) that second-minimum location was a critical dimension. To explore this variable further, both scoop configurations were moved toward the nozzle exit plane as indicated in configurations 3(b) and 1(d) (fig. 14), and a third scoop configuration (configuration 4) with an 8° scoop angle was included for evaluation at this position. The change in inlet location unavoidably changes two variables simultaneously, namely, free-jet length l_1 as well as distance to second minimum l_3; however, the influence of these individual variables can be separated to some degree by cross comparisons.

As summarized in figure 14, shortening the free-jet lengths produced a marked increase in running efficiency with models installed for both configurations, and for this shorter free-jet condition the two-stage scoop (configuration 3(b)) allowed operation with more severe blockage than the original 15° scoop (configuration 1(d)). The third scoop configuration (8° angle, configuration 4), on the other hand, had less efficiency with model installed although its efficiency (122 percent) for empty-jet condition was approximately equal to the other configurations. These results would indicate that for the empty-jet condition, scoop configuration and free-jet length have only moderate effects on operating efficiency for a system of this type. With blunt models in place, however, a marked system improvement was obtained when free-jet length was shortened to approximately one nozzle diameter ($l_1 = D_1$) and for this short free-jet condition the two-stage scoop (configuration 3(b)) exhibited the best model operating capability of the three scoops evaluated. On the basis of these tests the two-stage scoop with free-jet length of D_1 (configuration 3(b)) was chosen for use in the remainder of this investigation.

Effect of length of second minimum.- The effect of varying the length of second-minimum section in the diffuser was evaluated by using configurations 3(b), 3(c), and 3(d) (fig. 4 and table I) which combined the scoop and second-minimum area ratio configurations found best in the previous studies. The results of these tests are summarized in figure 15 and show that increasing the length of second-minimum section from 1.9 to 6.3 local diameters increased the system efficiency approximately 14 percent for the empty-jet condition and approximately 21 percent for the most severe model condition. The major gains were obtained for length increases from 1.9 to approximately 4 diameters, and only minor increase in efficiency occurred beyond this point. Some additional tests were made for these configurations with the 2° conical tailpipe removed from the system. For this condition the effect of reducing length of the second-minimum section was much more pronounced and, although the tunnel could still be operated, marked reductions in operating efficiency occurred for all cases.

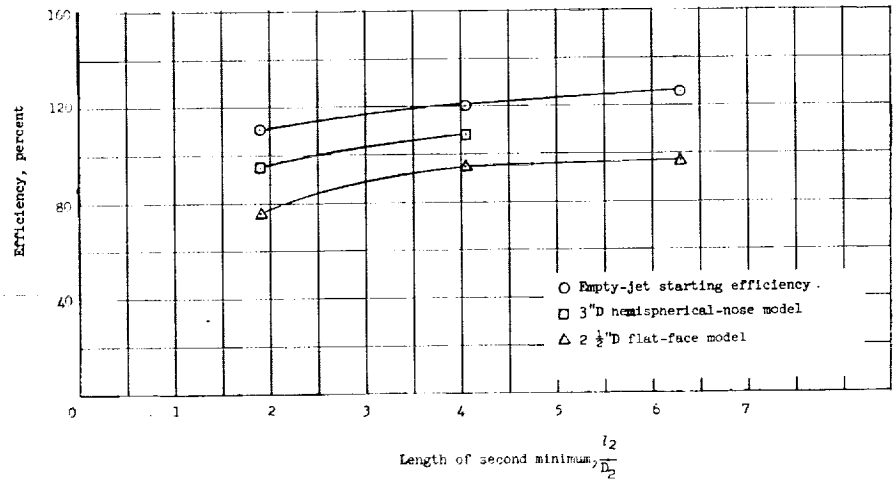

Figure 15.- Effect of second-minimum length on diffuser efficiency for configurations 3(b), 3(c), and 3(d).

The results of these tests generally confirm the concept that the most efficient diffusion process for this type of system is largely a mixed-flow process in the straight-pipe section; static pressure distributions (figs. 16 and 17) measured in diffuser configuration 3(b) further illustrate this concept. Although other length combinations of second minimum and tailpipe sections

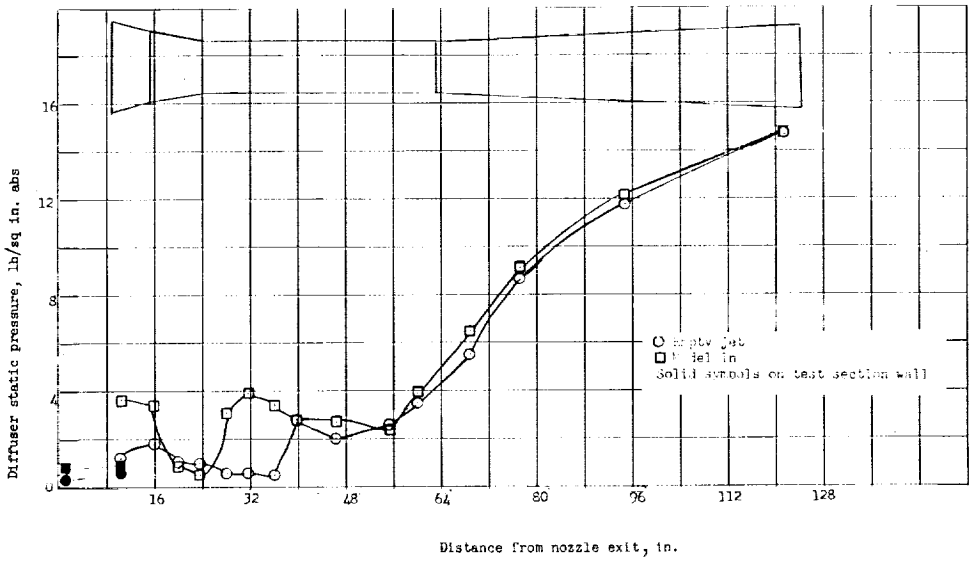

Figure 16.- Static pressure distribution along diffuser with no model and with 3"D hemispherical-nose model (configuration 3(b)). T_o, 2,915° F; p_o, 800 lb/sq in.

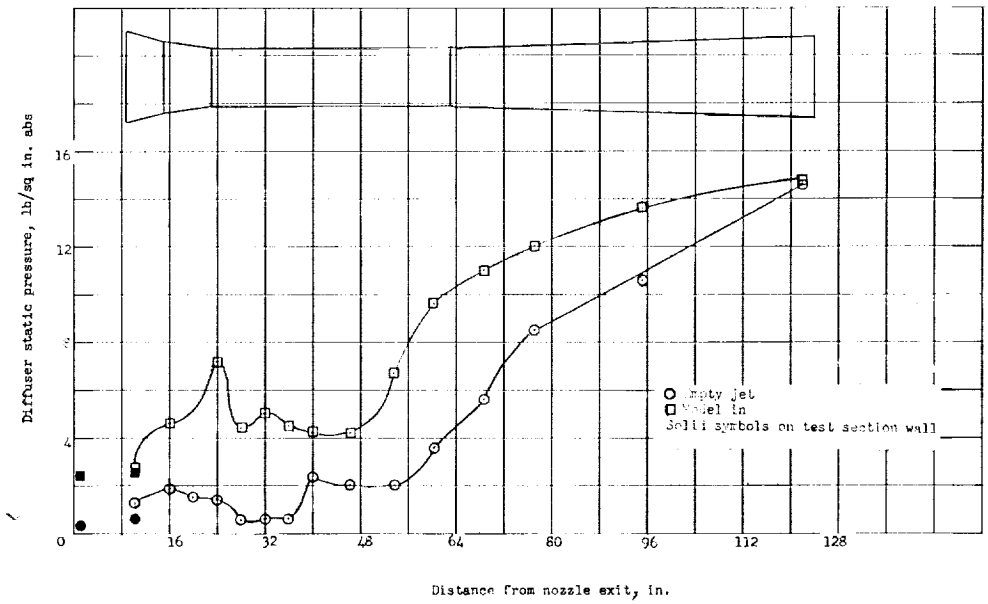

Figure 17.- Static pressure distribution along diffuser with no model and with $2\frac{1}{2}$" D flat-face model (configuration 3(b)). T_o, 2,780° F; p_o, 800 lb/sq in.

probably could have been used to provide the mixing length required, this diffuser was finalized by using the 4-diameter $4D_2$ length second-minimum section with the original 2° conical tailpipe (configuration 3(b)).

Performance of Final Diffuser Configuration

Configuration 3(b) was selected for the Mach 6 diffuser because it had acceptable efficiency for a wide range of models. The operational capability of the tunnel with configuration 3(b) is summarized in figure 18 and table II

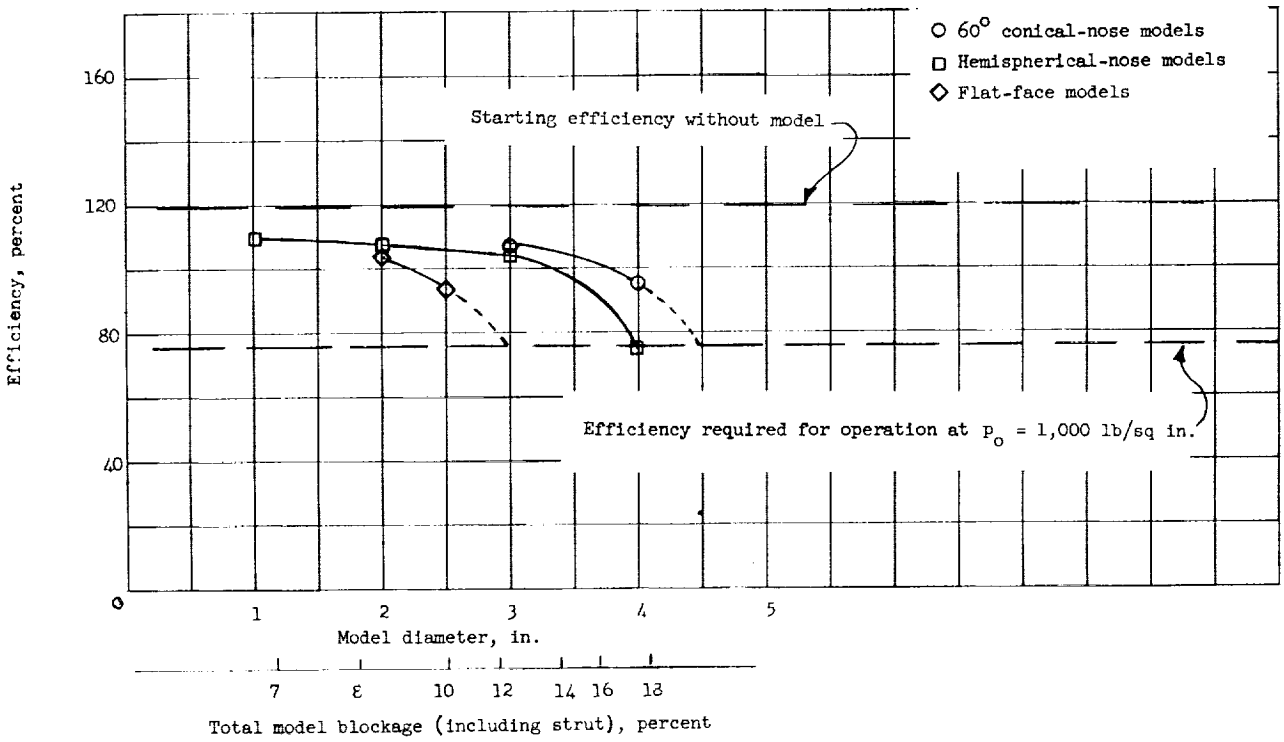

Figure 18.- Effects of model blockage on diffuser efficiency for best configuration tested (configuration 3(b)).

for three types of models of interest in materials-evaluation test work. The tunnel could be started at a stagnation pressure of 630 lb/sq in. abs corresponding to an efficiency of 120 percent. Within the nominal 1,000 lb/sq in. abs stagnation-pressure limit of the system the tunnel could accommodate hemispherical and 60° conical nose models up to 4 inches in diameter which corresponds to a blockage area (including strut) of 17.9 percent of jet area. The 4-inch conical model could be operated at a higher efficiency than the hemisphere; however, the tunnel could not be operated with a $4\frac{1}{2}$-inch-diameter conical model within the 1,000 lb/sq in. abs stagnation limit. With flat-face models, a 3-inch-diameter model could not be operated at maximum pressure; however, with the model face chamfered to leave a $2\frac{1}{2}$-inch flat face (fig. 5, model 7) flow was maintained without difficulty.

For the final tunnel configuration, tests have been made with various models installed for tunnel stagnation temperatures ranging from 70° F (cold flow) to 3,600° F (the design maximum for the system); no significant effects of temperature on operating characteristics have been observed. Also, tests made to check effects of techniques of model insertion and model location in the airstream did not indicate sensitivity to these variables. Models could be run equally well in on- or off-center positions over a range of longitudinal locations in the test section.

Test-Section Flow Studies

Typical flow photographs for the tunnel operating with various test models are shown in figure 19 where it can be seen that for all model conditions the

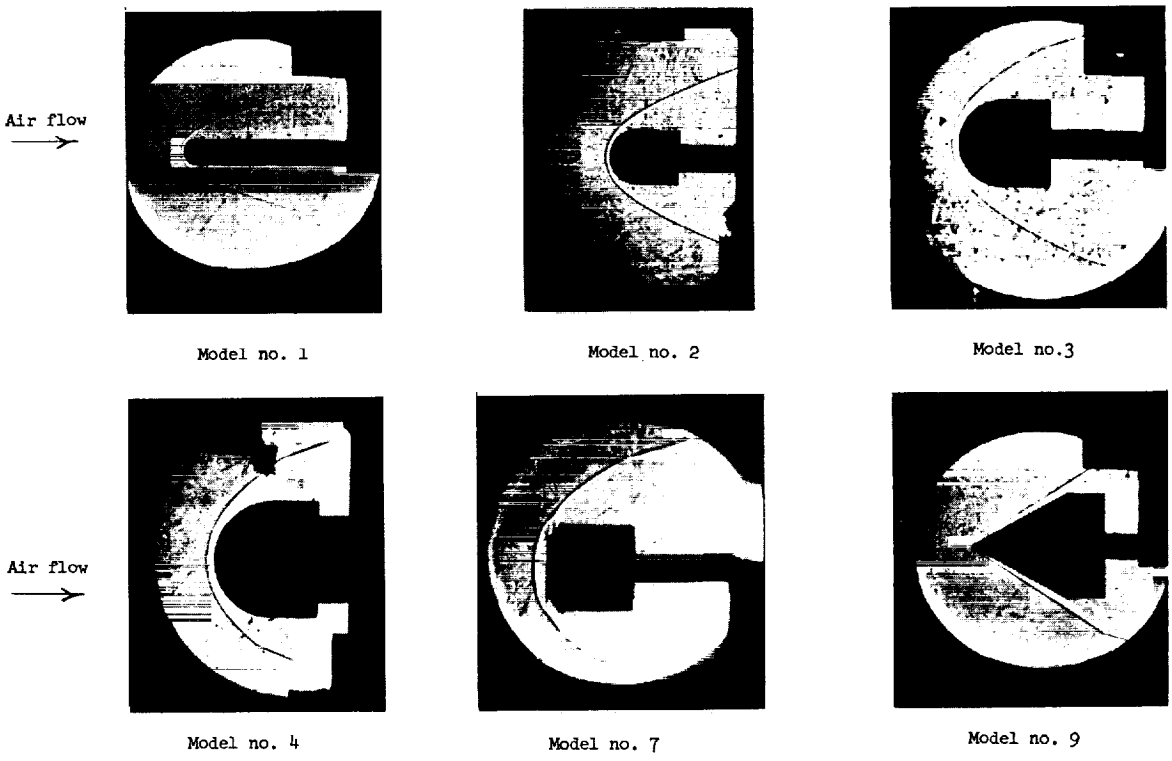

L-64-3028

Figure 19.- Typical shadowgraphs of several different models running with diffuser configuration 3(b) installed.

tunnel flow develops a boundary shock which increases in angle and strength with more severe blockage. This shock, which characterized the starting and stopping process in the tunnel (figs. 8 and 12), accompanies an increase in test-section static pressure to values somewhat higher than stream static pressure when models are inserted. For all conditions shown in figure 19, the boundary shock was stable and stagnation-pressure measurements on the blunt

models indicated that the flow in the test region was not appreciably affected by the boundary shock.

CONCLUSIONS

Consideration of the results of this program to evaluate diffuser configurations for a Mach 6 open-jet wind tunnel leads to the following conclusions:

1. The testing of blunt models in a tunnel with a fixed-geometry diffuser requires the use of a second-minimum area ratio appreciably larger than the optimum for empty-jet operation. An area ratio of 0.72 gave best model capability for the system of this study.

2. Shortening the tunnel free-jet length from 1.5 to 1.0 nozzle diameters gave a marked improvement in tunnel operating efficiency with blunt models installed but had little effect on empty-jet operation.

3. For the diffuser-scoop configuration studies, best model testing capability was obtained by using a two-angle (15° and 8°) inlet scoop positioned with a tunnel free-jet length of 1.0 nozzle diameter.

4. Increasing the length of the constant-area second-minimum section from 1.9 to 6 local diameters increased tunnel operating efficiency approximately 21 percent with models in place. The major gain was achieved for the length increases up to the 4-diameter value.

5. For the best diffuser developed in this program, hemispherical and 60° conical models with blockage areas of 14.2 percent (17.9 percent including struts) can be operated at diffuser efficiencies of 76 and 95 percent, respectively.

6. Tunnel stagnation temperature did not have an appreciable effect on diffuser operating characteristics within the range of this study (70° F to $3,600^\circ$ F).

Langley Research Center,
National Aeronautics and Space Administration,
Langley Station, Hampton, Va., March 17, 1964.

REFERENCES

1. Lee, John D., and Von Eschen, G. L.: Preliminary Studies, Design and Theory, for the Ohio State University Hypersonic Wind Tunnel. Tech. Rep. No. 1 (Contract DA-33-019-ORD-1634), Ohio State Univ. Res. Foundation, Aug. 1956.

2. Trout, Otto F., Jr.: Design, Operation, and Testing Capabilities of the Langley 11-Inch Ceramic-Heated Tunnel. NASA TN D-1598, 1963.

3. Ames Research Staff: Equations, Tables, and Charts for Compressible Flow. NACA Rep. 1135, 1953. (Supersedes NACA TN 1428.)

4. Liepmann, H. W., and Roshko, A.: Elements of Gasdynamics. John Wiley & Sons, Inc., c.1957, pp. 124-138.

5. Thomas, R. E.: The Starting Process of a Free-Jet Hypersonic Wind Tunnel. Aerod. Lab. Tech. Memo. No. 14, Ohio State Univ., Sept. 1958.